

# Importance of contraction history on muscle force of porcine urinary bladder smooth muscle

Robin Menzel<sup>1</sup> · Markus Böl<sup>2</sup> · Tobias Siebert<sup>1</sup>

Received: 28 October 2016 / Accepted: 7 December 2016 / Published online: 17 December 2016  
© Springer Science+Business Media Dordrecht 2016

## Abstract

**Introduction** The purpose of this study was to provide a comprehensive dataset of porcine urinary bladder smooth muscle properties. Particularly, the history dependence of force production, namely force depression (FD) following shortening and force enhancement (FE) following stretch, was analysed. During active micturition, the circumference of the urinary bladder changes enormously. Thus, FD might be an important phenomenon during smooth muscle contraction.

**Materials and methods** Electrically stimulated, intact urinary bladder strips from pigs ( $n = 10$ ) were suspended in an aerated-filled organ bath, and different isometric, isotonic, and isokinetic contraction protocols were performed to determine the force–length and the force–velocity relation. FD and FE were assessed in concentric and eccentric contractions with different ramp lengths and ramp velocities.

**Results** Bladder smooth muscles exhibit considerable amounts of FD and FE. The amount of FD increased significantly with ramp length, while FE did not change. However, FE and FD were independent of ramp velocity.

**Conclusion** The results imply that smooth muscle bladder strips exhibit similar muscle properties and history-dependent behaviour compared to striated muscles. The provided dataset of muscle properties is important for bladder modelling as well as for the analyses and interpretation of dynamic bladder filling and voiding.

**Keywords** Force depression · Force enhancement · Pig · Force–length relation · Force–velocity relation · Muscle properties

## List of symbols

Curv	Curvature factor
$F_{im}$	Maximum isometric muscle force
FD	Force depression
FE	Force enhancement
$L_{opt}$	Optimum muscle length associated with $F_{im}$
$L_{ramp}$	Ramp length
$L_s$	Slack length
$L_{start}$	Start length
$V_{max}$	Maximal shortening velocity

## Introduction

Muscles are the motors of life, and the determination of their properties is relevant for understanding muscle function and for development of realistic models. It is well-known that besides velocity of shortening, overlap between actin and myosin, and degree of activation [1–3], muscle force production depends also on its contraction history [4, 5]. Compared to the corresponding isometric muscle force at the same muscle, the force is enhanced in the isometric phase following active stretching (force enhancement, FE) and depressed following active shortening (force

✉ Robin Menzel  
robin.menzel@inspo.uni-stuttgart.de

Markus Böl  
m.boel@tu-braunschweig.de

Tobias Siebert  
tobias.siebert@inspo.uni-stuttgart.de

<sup>1</sup> Institute of Sport- and Movement Science, University of Stuttgart, Allmandring 28, 70569 Stuttgart, Baden-Württemberg, Germany

<sup>2</sup> Institute of Solid Mechanics, Technische Universität Braunschweig, 38106 Braunschweig, Niedersachsen, Germany

depression, FD). The two phenomena have been observed in situ for whole striated muscles [4, 6], isolated muscle fibres [7], and in vivo electrically stimulated human muscles [8]. The majority of studies examining history dependence of muscle force were performed using striated muscles. It was reported that FD increases with increasing shortening amplitudes and decreases with higher shortening velocities [4]. Moreover, FD is not directly related to the shortening velocity but rather to the exerted work during shortening, which changes as a function of speed [9]. FE is directly related to the amount of stretch and is almost independent of stretch velocity [10]. In striated muscles, the extent of FE and FD ranges up to 100% and 5–20% of the maximum isometric force ( $F_{im}$ ) [11], respectively.

The underlying mechanisms for these phenomena are not clearly understood [12]. Reasons that might explain FE are a conglomerate of sarcomere length non-uniformities [5], titin–actin interactions [13, 14], and modified cross-bridges kinetics [7]. Potential mechanisms for FD range from disorganisation of sarcomeres and filaments [15], high cytoplasmic calcium concentrations after shortening, (re)attachment of cross-bridges [16], and titin–actin interactions [14].

The majority of studies who dealt with smooth muscles focused on muscle parameters like force–length [17–19] or force–velocity [17, 19, 20] relationships. Research regarding history dependence is quite rare, although the ability of smooth muscles to shorten is the most important attribute for transport or execution functioning. In sum, we only found two studies that examined FD in smooth muscles [16, 21]. Ramp length-dependent FD was reported for canine tracheal smooth muscles [21]. A high physiological relevance of FD is expected, especially for smooth muscles in the wall of hollow organs, such as the bladder, stomach, and intestine. For example, the circumference of the urinary bladder changes enormously during active micturition, which might induce large FD. In general, van Asselt et al. [16] found the effect of FD in smooth muscle bundles of urinary bladders from pigs. By varying their length and velocity simultaneously, no clear characterisation of length and velocity dependence of FD was detected. Thus, a quantitative comparison with skeletal muscles [4] or the determination of FD model parameters is not possible [22].

To the best of the authors knowledge, to date FE has not been examined for smooth muscles. Physiological relevance of FE seems negligible in view of predominantly concentric contractions during active micturition of urinary bladders. However, pathological obstructions after prostatic hyperplasia or bladder cancer could induce active muscle stretching [23] and consequently, FE. Furthermore, recent modelling studies suggested similar mechanisms for FE and FD in skeletal muscles [14, 24–26]. Thus, characterisation of both phenomena in smooth muscles enables

comparison with striated muscles, having similar principles of actin–myosin-based active force generation as smooth muscles but differ in the sarcomere structure [12, 27]. Also, this characterisation might contribute to a better understanding of the history dependence in smooth muscles.

Hence, the aim of this study is to characterise the length and velocity dependence of FE and FD in smooth muscle tissue. To achieve this goal, we performed in vitro stretching and shortening experiments with porcine bladder tissue strips. To enhance the set of muscle properties, e.g. for modelling studies, essential muscle properties (force–length and force–velocity relations) were also determined.

## Materials and methods

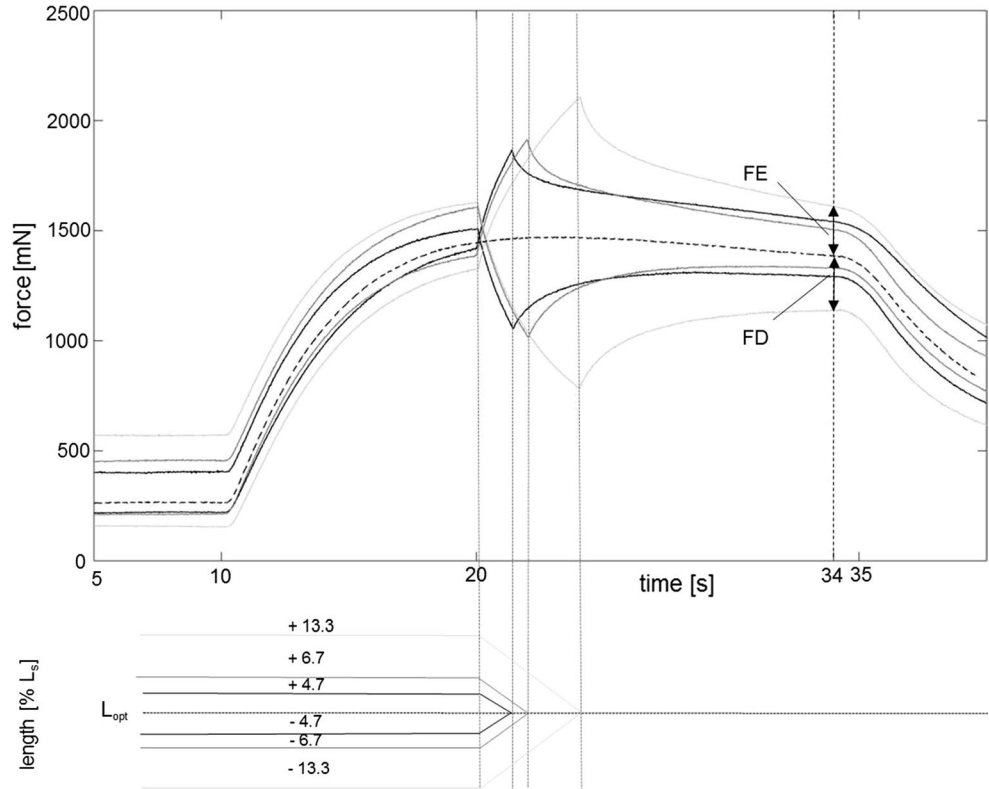
### Handling and preparation

Experiments were approved according to section 8 of the German animal protection law (Tierschutzgesetz, BGBI. I 1972, 1277). The urinary bladders of 10 healthy and freshly killed female pigs (approximately 6 months and 100 kg) were collected from the local slaughterhouse and prepared within 60–90 min after the death of the pig. The bladder tissue was kept in a modified Krebs solution (25 mM  $\text{NaHCO}_3$ ; 1.2 mM  $\text{NaH}_2\text{PO}_4$ ; 2.4 mM  $\text{MgSO}_4$ ; 5.9 mM  $\text{KCl}$ ; 2.5 mM  $\text{CaCl}_2$ ; 117 mM  $\text{NaCl}$  and 11 mM  $\text{C}_6\text{H}_{12}\text{O}_6$  [28]) aerated with 95%  $\text{O}_2$  and 5%  $\text{CO}_2$  (pH 7.4) at a constant temperature of 4 °C. The bladder was opened through the Ligamentum vesicae medianum and a longitudinal strip ( $0.83 \pm 0.2$  g) of  $18 \times 10$  mm was cut from the dorsal cranial surface of the bladder wall. The strip was fixed between a clamp with penetration pins and two flexible cannula hooks on the bottom. The clamp was connected with a surgical suture (Maprolen 2  $\times$  DRE 13, 5/0, Catgut GmbH) to a Dual Mode Lever Arm System (Aurora Scientific 305C-LR, force range: 10 N, force resolution: 1 mN). The data acquisition and processing was obtained by a signal interface (Aurora Scientific 604A) and fed into a computer via an A/D converter. The stimulation and mechanical setup were software-controlled (Aurora Scientific 610A). Length changes of the strip were realised due to vertical movement of the lever (range of motion = 16 mm). The slack length ( $L_s$ ) of the strip between the clamp and the two hooks was 15 mm. The experiments were performed in an organ bath (100 ml) filled with an aerated Krebs solution. The temperature was kept constant at 37 °C by water circulation. Strips were activated by applying bi-polar pulses via two platinum field electrodes ( $65 \times 2$  mm) placed at each side of the strip. Alternating pulses of 900 mA, 100 Hz, 5 ms [28] were generated by a high-power biphasic pulse Stimulator (Aurora Scientific 701C) to achieve maximal forces.

**Table 1** Specification of muscle properties determined for each urinary bladder tissue strip

Strip number	S1	S2	S3	S4	S5	S6	S7	S8	S9	S10
Force–length relation	x	x	x	x	x	x	x	x	x	x
Force–velocity relation	x	x	x	x	x	x	x			
FD	x	x	x	x	x	x	x	x		
FE	x	x	x	x	x	x	x			

**Fig. 1** FE and FD experiments with varying ramp length. Force–time (*upper figure*) and length–time traces (*lower figure*) of isometric–shortening–isometric and isometric–lengthening–isometric experiments (strip number S6) performed at a given velocity (20%  $v_{max}$ ). Ramps started from different lengths (13.3, 6.7, 4.7%  $L_s$ ) and were finished at the same final length ( $L_{opt}$ , *black dotted line*). Stimulation started at  $t = 10$  s and was maintained up to  $t = 34$  s. FE and FD are the force difference between ramp experiment (*grey solid lines*) and isometric reference contraction (*black dotted line*) calculated 10 s after the ramp end (shown exemplarily for the longest ramp by *thick arrows*)



After an equilibration period of 30 min at  $L_s$ , the strip was stimulated isometrically every 7 min until the active force was stable (deviation  $< 5\% F_{im}$ ). Experiments were performed at intervals of 7 min to avoid muscle fatigue effects.

**Protocol**

Isometric, isotonic, and isokinetic experiments have been performed to determine muscle properties [29] (force–length and force–velocity relations, FD, FE) using 10 urinary bladder smooth muscle strips in total (Table 1).

The force–length relationship was investigated by a series of 13 isometric contractions with increasing muscle length. Muscle length at  $F_{im}$  was defined as the optimum muscle length ( $L_{opt}$ ). A series of isotonic contractions starting at  $L_{opt}$  against forces of 0.1–0.9  $F_{im}$  was performed [30] to identify the force–velocity relation which was fitted by the typical hyperbolic Hill equation

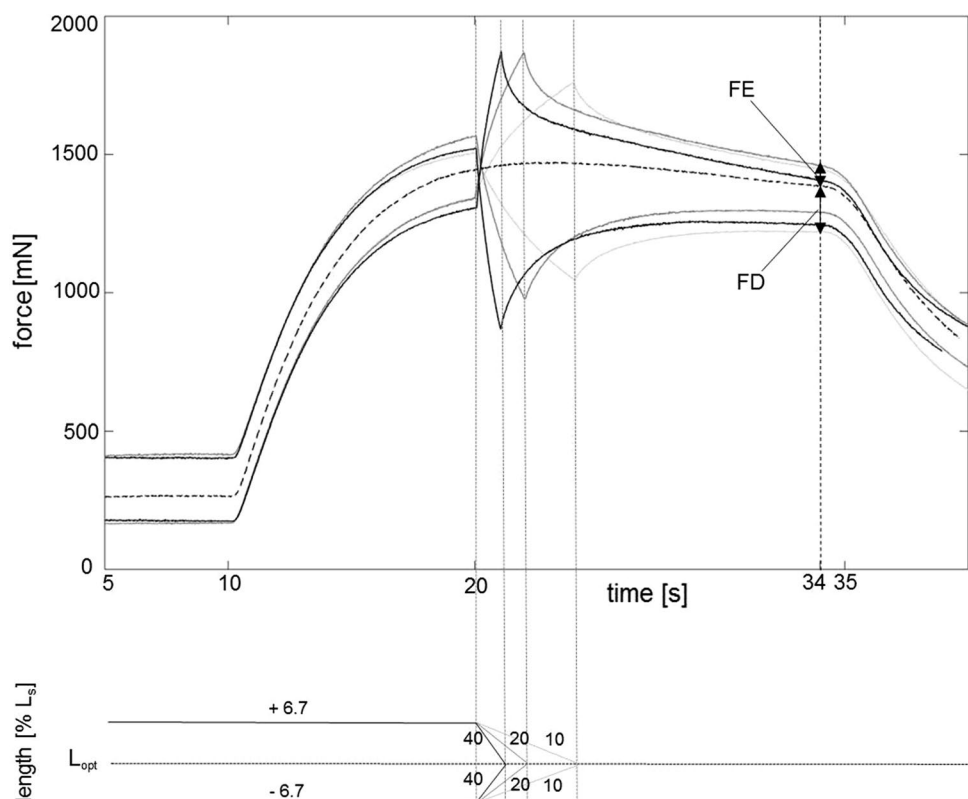
$$f(v) = \frac{v_{max} - v}{v_{max} + v/curv} \quad v < 0, \tag{1}$$

for concentric contractions. Herein,  $v_{max}$  is the maximal shortening velocity and  $curv = a/F_{im}$  (the parameter  $a$  describes the force asymptote of the  $f(v)$  relation) denotes the curvature factor [1, 29].

The isokinetic ramp measurements were taken in the plateau range of the force–length relation. They started at the end of the ascending limb or the beginning of the descending limb for determination of FE and FD, respectively. Isokinetic ramps were finished at  $L_{opt}$  (Figs. 1, 2).

Strips ( $n = 8$ ) were stretched passively to an initial length  $L_{start} = L_{opt} \pm L_{Ramp}$ , where  $L_{Ramp}$  is the ramp length. Once the steady-state isometric force was reached (approximately 10 s after stimulation), the dependency of contraction history on ramp length was examined in a first series of experiments (Fig. 1). Therefore, strips were extended/shortened to  $L_{opt}$  at a given speed (20%  $v_{max}$ ) by varying stretch amplitudes

**Fig. 2** FE and FD experiments with varying ramp velocities. Force–time (*upper figure*) and length–time traces (*lower figure*) of isometric–shortening–isometric and isometric–lengthening–isometric experiments (strip number S6) performed with varying velocities (10, 20, 40%  $v_{\max}$ ). Ramps started at a given initial length ( $\pm 6.7\%$   $L_{\text{opt}}$ ) and were finished at the same final length ( $L_{\text{opt}}$ , *black dotted line*). Stimulation started at  $t = 10$  s and was maintained up to  $t = 34$  s. FE and FD are the force difference between ramp experiment (*grey solid lines*) and isometric reference contraction (*black dotted line*) calculated 10 s after the ramp end (shown exemplarily for the slowest (34 s) ramp by *thick arrows*)



(4.7, 6.7, and 13.3%  $L_s$ ). In a second series of experiments, the dependency of contraction history on ramp velocity was examined (Fig. 2) by variation of ramp velocities (10, 20, and 40%  $v_{\max}$ ) at a given ramp length (6.7%  $L_s$ ). For calculating FE and FD, isometric reference contractions at  $L_{\text{opt}}$  were performed continuously before and after each ramp protocol. FE and FD were determined 10 s after the end of each ramp as the difference between the redeveloped and the corresponding purely isometric force at the same length normalised to  $F_{\text{im}}$ .

### Data processing and statistics

All data were sampled at 100 Hz by software (610A Dynamic Muscle Analysis, Aurora Scientific) and processed using MATLAB (The Mathworks, Inc., Natick, MA, USA). The data were expressed as mean  $\pm$  standard deviation. No indication for deviation from normal distribution was found by the Kolmogorov–Smirnov test with  $P > 0.05$  for all parameters. The Levené test was utilised to check variance homogeneity. A one-way ANOVA was used to determine significant differences ( $P < 0.001$ ) of FE and FD concerning length and velocity dependence. If they demonstrated that the significant main effects and variances were homogenous, post hoc analyses were performed using the Tukey HSD test. For inhomogeneous variances, we used the Dunnett C test. Statistical analyses were realised using SPSS 22 (IBM Corp, Armonk, NY, USA).

### Determination of smooth muscle cross-sectional area

Smooth muscle cross-sectional areas (Fig. 3) were determined from digital pictures of cryo-histological sections of bladder smooth muscle strips. In doing so, dissected specimens were fixed on cork plates and flash frozen in isopentane at  $-160$  °C, which in turn was cooled at  $-210$  °C using nitrogen. Using a cryomicrotome, 10-mm-thick slices were sectioned and thereafter stained with Van Gieson stain for microscope analysis. Finally, sections were analysed using a digital microscope (Zeiss Smartzoom 5), allowing the recording of full-size images and thus the determination of wall thicknesses.

In accordance with Fig. 3, the tunica muscularis of the bladder wall features two sublayers (inner tunica muscularis, outer tunica muscularis [31]). After analysing various sections, at this point, we would like to note that the aforementioned arrangement is strongly dependent on the wall position and further on the individual bladder.

### Results

The force–length relation of bladder muscle strips exhibits an ascending limb, a plateau region, and a descending limb (Fig. 4).

The maximum isometric force at  $L_{\text{opt}}$  is  $1391.9 \pm 280.9$  mN ( $n = 10$ ) and corresponds to a maximal

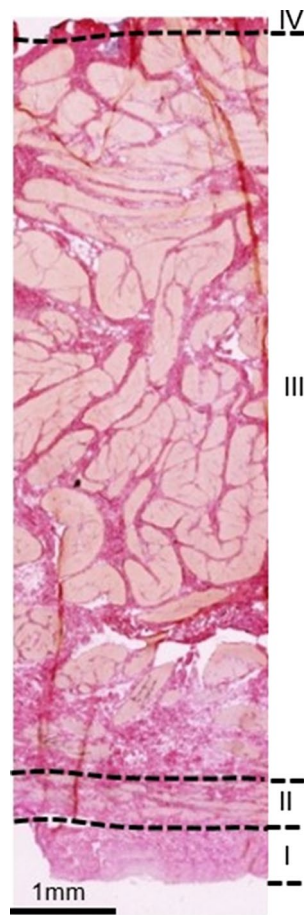


**Fig. 3** Section of a typical porcine urinary bladder strip. Four different regions can be identified: *I* tunica mucosa, *II* tunica propria, *III* tunica muscularis, and *IV* tunica adventitia. Typically, tunica muscularis of humans are composed of three smooth muscle layers (inner longitudinal, middle circular, outer longitudinal) [23]

tension of  $3.40 \pm 0.73 \text{ N/cm}^2$ . A sector of the muscle cross-sectional area of a typical urinary bladder smooth muscle strip is shown in Fig. 3. Usually, pig tunica muscularis consist of two not clearly delimitable smooth muscle layers (inner and outer muscularis).

$L_{\text{opt}}$  was found in the range between 2.6 and 2.8  $L/L_s$  (length of the strip,  $L$ ). Passive forces at  $L_{\text{opt}}$  range from 20 to 50%  $F_{\text{im}}$ . Interestingly, the bladder strip generates only minor active force (10%  $F_{\text{im}}$ ) at  $L_s$ . Maximal muscle shortening exemplarily shown in Fig. 4 was reached slightly below  $L_s$  ( $0.82 \pm 0.17 L/L_s$ ). To avoid muscle damage, the bladder strips were lengthened until passive forces  $<0.8 F_{\text{im}}$  (Fig. 4). The force decreased linearly with increasing muscle length on the descending limb of the force–length relation. Extrapolation of this linear decrease yielded zero force at approximately  $4.94 \pm 1.24 L_s$ . Bladder smooth muscle strips exhibit a typical hyperbolic force–velocity relation (Fig. 5). The maximal shortening velocity is

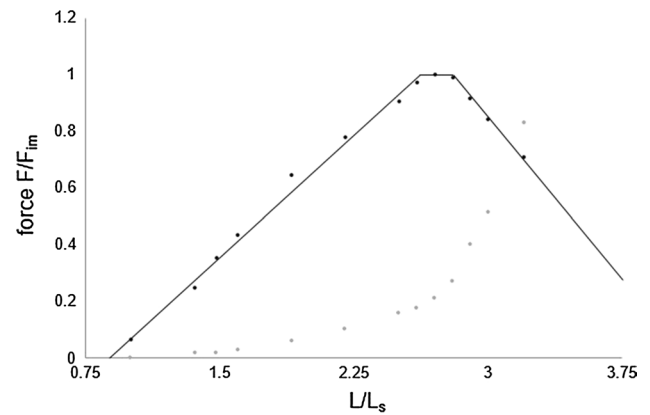


**Fig. 4** Force–length relation from urinary bladder smooth muscle strip (S6). Active isometric force (black circles) and passive force (grey circles) as function of muscle length.  $F_{\text{im}}$  is the maximum isometric muscle force,  $L_s$  is the slack length of the strip. The ascending ( $f_1$ ) and descending ( $f_2$ ) limb functions of the force–length relation are fitted by straight lines with the equations:  $f_1(x) = F/F_{\text{im}} = 0.58x - 0.51$  and  $f_2(x) = F/F_{\text{im}} = -0.71x + 2.98$ , where  $x = L/L_s$

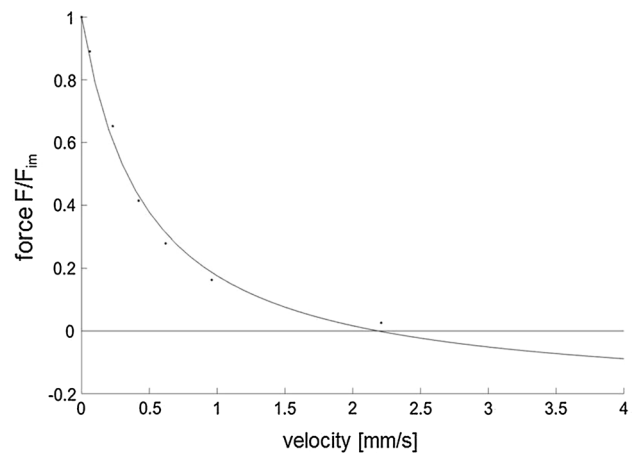


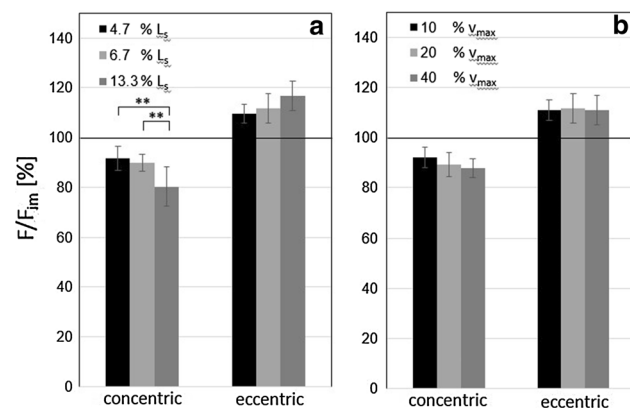
**Fig. 5** Force–velocity relation from urinary bladder smooth muscle strip (S6). The normalised force (black circles) as function of the velocity was calculated from a series of isotonic contractions. The hyperbolic black curve shows the typical Hill equation [1], with  $a/F_{\text{im}} = \text{curv} = 0.22$ ,  $b = 0.48 \text{ mm/s}$  ( $a$  describes the force asymptote,  $b$  the velocity asymptote) and  $v_{\text{max}} = 2.19$  (the intersection of the fitted hyperbolic curve with the velocity–axis)

$2.49 \pm 0.37 \text{ mm/s}$  ( $n = 7$ ), and the curv value of the force–velocity relation is  $0.27 \pm 0.08$  (Fig. 5).

A summary of FD and FE for all experiments is shown in Table 2. Forces were significantly ( $P < 0.05$ ) depressed/enhanced following 4.7, 6.7 and 13.3 (%  $L_s$ ) ramp lengths and 10, 20, 40 (%  $v_{\text{max}}$ ) ramp velocities compared to the corresponding isometric force (Fig. 6a). The amount of FD was directly related to the amount of shortening. For

**Table 2** Mean  $\pm$  standard deviations of depressed (FD) and enhanced forces (FE) after different ramp experiments

	(% $F_{im}$ )	$n$	$P$
<i>Force depression (FD)</i>			
Ramp length (% $L_s$ )			
4.7	6.55 $\pm$ 4.62	7	0.00 †#
6.7	8.40 $\pm$ 3.35	7	
13.3	17.93 $\pm$ 7.01	7	
Ramp velocity (% $v_{max}$ )			
10	7.48 $\pm$ 3.70	7	ns
20	8.40 $\pm$ 3.35	7	
40	10.18 $\pm$ 3.13	8	
Mean	8.54 $\pm$ 3.57	22	
<i>Force enhancement (FE)</i>			
Ramp length (% $L_s$ )			
4.7	8.29 $\pm$ 3.64	7	ns
6.7	10.21 $\pm$ 5.48	7	
13.3	11.70 $\pm$ 5.76	7	
Ramp velocity (% $v_{max}$ )			
10	7.32 $\pm$ 2.82	7	ns
20	10.21 $\pm$ 5.48	7	
40	7.80 $\pm$ 7.80	7	
Mean	8.45 $\pm$ 5.59	21	

Significant differences ( $P < 0.01$ )ns means no significant and  $n$  is the number of samples† Between 4.7 and 13.3%  $L_s$ , # between 6.7 and 13.3%  $L_s$ **Fig. 6** Dependency of contraction history (FD and FE) on ramp length and ramp velocity. Forces were normalised to  $F_{im}$ . Mean forces  $\pm$  standard deviations were given. **a** Ramp length was varied (black: 4.7%  $L_s$ , light grey: 6.7%  $L_s$ , dark grey: 13.3%  $L_s$ ) at constant ramp velocity (20%  $v_{max}$ ). **b** Ramp velocity was varied (black: 10%  $v_{max}$ , light grey: 20%  $v_{max}$ , dark grey: 40%  $v_{max}$ ) at constant ramp length (6.7%  $L_s$ ). Forces after ramp perturbation differ significantly ( $P < 0.05$ ) from isometric force (black straight line). Significance: \*\* $P < 0.01$ 

the longest ramp (13.3%  $L_s$ ), FD was approximately two-fold (17.9%  $F_{im}$ ) compared to the shorter ramp lengths (6.6 and 8.4%  $F_{im}$  for 4.7 and 6.7%  $L_s$ , respectively;  $P < 0.01$ ).

FE increased by trend but not significantly with increasing magnitudes of stretch (Fig. 6a; Table 2). FE induced by the longest and shortest ramp was 11.7 and 8.29%  $F_{im}$ , respectively. Our data indicate that FD (approximately 8.54  $\pm$  3.57%  $F_{im}$ ) and FE (approximately 8.45  $\pm$  5.59%  $F_{im}$ ) were statistically independent on ramp velocity (Fig. 6b).

## Discussion

### Bladder muscle properties: Comparison with literature

Mean muscle tension of urinary bladder smooth muscle (3.40  $\pm$  0.73 N/cm<sup>2</sup>) is in the range (2.5–6.0 N/cm<sup>2</sup>) of other pig bladder studies [20, 28] but reduced by a factor of 2–3 compared to maximal muscle tension reported for small mammal urinary bladders [32]. A maximum shortening velocity of 0.1  $L_{opt}/s$  is in accordance with values of 0.1–0.5  $L_{opt}/s$  reported for mammalian smooth muscle [19, 33]. However,  $v_{max}$  is lower by about one order of magnitude compared to skeletal muscles [34–36]. The curve of 0.22 is in agreement with values reported for smooth muscle [19]. Further, similar values can be found for skeletal muscles, reaching from 0.1 to 0.5 [29].

Starting from slack length ( $L_s$ ), the maximum isometric force was reached after large elongations of the muscle strip as reported in [37], i.e.  $L_{opt} = 290 \pm 68\%$   $L_s$ . Normalising the force–length relation of the bladder strip to  $L_{opt}$ , the classic length for zero force (at the start of the ascending limb) is located in the range of 0.5–0.6  $L_{opt}$  similar to striated muscles [29, 38]. For prolonged stimulus durations, skeletal muscles are able to shorten much further [3, 39, 40]. However, due to usage of constant stimulus durations (12 s) for the analysis of the smooth muscle force–length relation, this issue was not addressed in the present study.

Although the general shape of the smooth muscle force–length relationship (Fig. 4) was similar to that of skeletal muscles [29, 38], indicating a similar force generating process driven by cross-bridge interaction, there are several differences. In contrast to the typical skeletal muscle force–length relation [38], no clear slope change at the ascending limb of bladder muscle force–length relationship was found (Fig. 4). In striated muscles, featuring a regular arrangement of myofilaments, the slope change appears at a sarcomere length where all myosin filaments reach the Z-disc (at 1.6  $\mu$ m in mammals) and was explained by myosin filament sliding through the meshed Z-disc [3]. Smooth muscles have no Z-disc, but the actin filaments of the contractile units are attached to dense bodies. Thick myosin filaments are side polar without any central bar zone. Furthermore, they show an extremely variable arrangement of muscle fibres in bundles of variable length, cross-section, and orientation, forming

a three-dimensional meshwork [41]. These structural differences might lead to differences in force generation, especially at the ascending limb of the force–length relation.

With reference to its slack length, bladder muscles exhibit a much larger working range ( $3.3 L_s$  corresponding to shortening from 4.1 to  $0.82 L_s$ , Fig. 4) compared to skeletal muscles (about  $1.2 L_s$ , [42]). This might be due to much higher  $L_{opt}/L_s$  ratio in bladder muscles ( $\approx 3$ ) compared to that of striated muscles (1–1.2, [43]), which enables huge elongations beginning at rest length and more important large active muscle shortening during micturition after these large passive elongations. Large active muscle shortening might be facilitated by differences in the myofibrillar microstructure. Bladder muscles exhibit longer myosin filaments ( $2.2 \mu\text{m}$ , [23]) compared to skeletal muscles ( $1.6 \mu\text{m}$ , [42]) which may contribute to a larger working range. However, this leads to less maximal shortening velocities. To better understand the functionality and contractile properties of the urinary bladder, a more detailed knowledge about anatomical and physiological properties of smooth muscle tissue is necessary.

### History dependence of bladder strips

The main findings of the present study indicate that the active force generated by bladder smooth muscles depends on contraction history. As reported for striated muscles, FE was independent of stretch velocity [44–46], and FD increased with ramp length [16, 21] but was independent of ramp velocity [9, 47, 48]. However, other studies reported that FD in skeletal muscles was inversely related to the speed of shortening [4, 29]. In contrast to Abbott and Aubert [4], no influence of ramp length on FE was observed, which might be ascribed to the insufficient variation in ramp length. Similar to other smooth muscle studies [16, 21], we used ramp lengths in the range of 4.7–13.3%  $L_s$ . However, due to the high  $L_{opt}/L_s$  ratio in bladder muscle (see “Bladder muscle properties: comparison with literature” section), this corresponds to much smaller ramp lengths (2–5%) with reference to  $L_{opt}$ . Although FE generally increases (Fig. 6a), this small variation in ramp length was not sufficient to induce a significant ramp length dependency (Table 2). Compared to experiments performed on striated muscles (FD: 10%  $F_{im}$  [49], FE: 5%  $F_{im}$ , [5]) using similar ramp lengths, we observed higher FD (17.9%  $F_{im}$ ) and higher FE (11.7%  $F_{im}$ ) (Table 2, longest ramp length).

The majority of studies examining history dependence of muscle force were performed on mammalian skeletal muscles. The reasons that might affect FE and FD are still a matter of debate [12]. FE in striated muscles has been suggested to relate to an increase in passive stiffness during and after stretching [14, 50]. This increase in stiffness might be caused by non-cross-bridge interactions,

more specifically by titin–actin interactions as proposed by the sticky–spring mechanism [14]. While intracellular  $\text{Ca}^{2+}$  concentration during activation increases, the PEVK region of titin, which is rich in proline (P), glutamic acid (E), valine (V), and lysine (K) [51], attaches to actin, leading to a decrease in the persistence length of the titin spring and thus in enhanced titin forces during stretch resulting in FE [14, 52]. The same phenomenon might contribute to FD in skeletal muscles as the titin spring is pulled in the other direction during muscle shortening, producing passive forces that act opposite to the active forces [14, 24]. Also, current research on striated muscles suggested a mechanism involving inhibition of cross-bridge binding to explain FD [53].

So far, it is unclear whether or not these explanatory approaches are applicable to smooth muscles since there are relevant differences in smooth muscles structure compared to striated muscles (see also “Bladder muscle properties: comparison with literature” section). Smooth muscles contract in a similar manner as other muscle types due to the interaction of actin and myosin filaments, although some rate constants are slower [54]. The contractile units are bounded on each end by dense plaques attached to the cell membrane or dense bodies distributed in the cell. Thereby, dense bodies act as equivalents to the Z-discs in striated muscles, but there are no titin filaments in smooth muscles. However, a protein with an amino acid composition similar to titin was isolated from a chicken gizzard smooth muscle [55]. The protein named smitin [56] exhibits a similar molecular morphology as well as the ability to interact with actin as reported for skeletal muscle titin [57–59]. In contrast to titin (molecular mass  $\sim 3.000$  kD and length  $>1 \mu\text{m}$ ), the molecular mass ( $\sim 2.000$  kD) and the length (750–900 nm) of smitin [56] are different [60]. Assuming a smitin–actin interaction in smooth muscles similar to the titin–actin interaction in striated muscles, the sticky–spring mechanism [14] might explain FD and FE in smooth muscles as well. We suggest that the differences in length and structure of titin and smitin or even different isoforms might contribute to the observed differences in contraction history between smooth and striated muscles. This is supported by Joumaa et al. [61], suggesting effects of different titin isoforms on the amount of FD in striated muscles. However, further studies investigating the interaction and structure of myofilaments during contraction are required to better understand history effects in smooth muscles.

### Physiological relevance

From a physiological point of view, history-dependent effects will influence the “behaviour” of hollow organs considerably. The two main bladder functions are storage

and voiding of urine. It has been shown that the duration of voiding did not vary among animals heavier than 3 kg. Based on the “Law of Urination”, animals completely empty their bladder content over a nearly constant duration of  $21 \pm 13$  s [62]. Additionally, mammals start to void when the bladder is nearly full [63]. Our results suggest that bladder voiding induced by concentric contraction will result in decreased muscle forces due to force depression and the influence of the force–length relation. Short interruption of urine flow by voluntary activation of the striated pelvic floor muscles results in an isovolumetric detrusor contraction and an increase in intravesical pressure [64]. The stopped voiding process leads to a decrease in bladder pressure as well as bladder smooth muscle deactivation, which may allow the muscle to recover [64]. Muscle deactivation has been shown to abolish FD [49]. Therefore, voluntary interruption of urine flow may be used to facilitate complete bladder emptying [64]. However, the possible influence of FD on limited bladder micturition and the physiological relevance of history effects in smooth muscles have to be addressed in future studies on whole bladders.

### Relevance of history effects regarding to model development

Besides the general enhancement of the physiological understanding of history effects in smooth muscle tissues, the presented data can also be helpful for the development of more comprehensive, numerical models. Traditional models that are able to simulate the active excitation behaviour of smooth muscle tissue [65–67] do not consider history effects. The consideration of such effects could improve the prediction accuracy. However, in addition information such as location-dependent smooth muscle fascicle and collagen fascicle orientations, the layer-specific active/passive characteristics, information about the innervation characteristics, and the link to whole organ mechanics to successfully describe the contraction behaviour of bladder wall tissue using a numerical model are still missing.

### Conclusion

This is the first study that provides a more comprehensive set of bladder smooth muscle properties, including the characterisation of contraction history after muscle shortening and lengthening. Despite obvious differences in bladder structure compared to striated muscles, similar contractile characteristics (e.g., force–length relation, force–velocity relation) and similar amounts of FE and FD as reported for striated muscles were found. Transfer of existing

explanatory approaches for history dependence of striated muscle forces requires further investigation of bladder microstructure, especially with regard to the influence of smitin on contraction dynamics. The results contribute to a better understanding of bladder function and are a precondition for modelling hollow organs like the urinary bladder.

**Acknowledgements** This work was funded by the Deutsche Forschungsgemeinschaft (DFG) under Grants BO 3091/9-1 and SI 841/9-1.

**Author’s contribution** TS and MB conceived and designed the experiments. RM performed the experiments, analysed the data and contributed reagents/materials/analysis tools. RM, MB, and TS wrote the paper.

### Compliance with ethical standards

**Conflict of interest** The authors declare that there are no conflicts of interest or future conflicts regarding this article.

**Ethical approval** All applicable international, national, and institutional guidelines for the care and use of animals were followed.

### References

- Hill AV (1938) The heat of shortening and the dynamic constants of muscle. *Proc R Soc B Biol Sci* 126:136–195
- Huxley AF (1957) Muscle structure and theories of contraction. *Prog Biophys Chem* 7:255–318
- Rode C, Siebert T, Tomalka A, Blickhan R (2016) Myosin filament sliding through the Z-disc relates striated muscle fibre structure to function. *Proc Biol Sci* 283:10–13
- Abbott BC, Aubert XM (1952) The force exerted by active striated muscle during and after change of length. *J Physiol* 117:77–86
- Edman KA, Elzinga G, Noble MI (1982) Residual force enhancement after stretch of contracting frog single muscle fibers. *J Gen Physiol* 80:769–784
- Lee HD, Herzog W (2002) Force enhancement following muscle stretch of electrically stimulated and voluntarily activated human adductor pollicis. *J Physiol* 545:321–330
- Linari M, Lucii L, Reconditi M, Casoni MEV, Amenitsch H, Bernstorff S, Piazzesi G, Lombardi V (2000) A combined mechanical and X-ray diffraction study of stretch potentiation in single frog muscle fibres. *J Physiol* 526(3):589–596
- De Ruiter CJ, De Haan A, Jones DA, Sargeant AJ (1998) Shortening-induced force depression in human adductor pollicis muscle. *J Physiol* 507:583–591
- Herzog W, Leonard TR, Wu JZ (2000) The relationship between force depression following shortening and mechanical work in skeletal muscle. *J Biomech* 33:659–668
- Rassier DE, Herzog W (2002) Force enhancement following an active stretch in skeletal muscle. *J Electromyogr Kinesiol* 12:471–477
- Campbell SG, Campbell KS (2011) Mechanism of residual force enhancement in skeletal muscle: insights from experiments and mathematical models. *Biophys Rev* 3:199–207
- Siebert T, Rode C (2014) Computational modeling of muscle biomechanics. In: Jin Z (ed) *Computational modelling of biomechanics and biotribology in the musculoskeletal system*, 1st edn. Woodhead Publishing/Elsevier, Amsterdam, pp 173–243



13. Rassier DE, Herzog W (2004) Effects of shortening on stretch-induced force enhancement in single skeletal muscle fibers. *J Biomech* 37:1305–1312
14. Rode C, Siebert T, Blickhan R (2009) Titin-induced force enhancement and force depression: A “sticky-spring” mechanism in muscle contractions? *J Theor Biol* 259:350–360
15. Edman K (1993) Depression of tetanic force induced by loaded shortening of frog muscle fibres. *J Physiol* 466:535–552
16. Van Asselt E, Pel JJM, van Mastrigt R (2007) Shortening induced effects on force (re)development in pig urinary smooth muscle. *J Biomech* 40:1534–1540
17. Griffiths DJ, van Mastrigt R, van Duyl WA, Coolseat BLRA (1979) Active mechanical properties of the smooth muscle of the urinary bladder. *Med Biol Eng Comput* 17:281–290
18. Uvelius B (2001) Length–tension relations of in vitro urinary bladder smooth muscle strips. *J Pharmacol Toxicol Methods* 45:87–90
19. Van Mastrigt R (2002) Mechanical properties of (urinary bladder) smooth muscle. *J Muscle Res Cell Motil* 23:53–57
20. Van Mastrigt R, Glerum JJ (1985) In vitro comparison of isometric and stop-test contractility parameters for the urinary bladder. *Urol Res* 13:11–17
21. Gunst SJ (1986) Effect of length history on contractile of canine tracheal smooth muscle. *Am J Physiol* 250:C146–C154
22. Kosterina N, Westerblad H, Eriksson A (2012) History effect and timing of force production introduced in a skeletal muscle model. *Biomech Model Mechanobiol* 11:947–957
23. Andersson K, Arner A (2004) Urinary bladder contraction and relaxation: physiology and pathophysiology. *Physiol Rev* 84:935–986
24. Schappacher-Tilp G, Leonard T, Desch G, Herzog W (2015) A novel three-filament model of force generation in eccentric contraction of skeletal muscles. *PLoS ONE* 10:1–16
25. Heidlauf T, Klotz T, Rode C, Altan E, Bleiler C, Siebert T, Röhrle O (2016) A multi-scale continuum model of skeletal muscle mechanics predicting force enhancement based on actin–titin interaction. *Biomech Model Mechanobiol*. doi:10.1007/s10237-016-0772-7
26. Nishikawa KC, Monroy JA, Uyeno TE, Yeo SH, Pai DK, Lindstedt SL (2012) Is titin a ‘winding filament’? A new twist on muscle contraction. *Proc Biol Sci* 279:981–990
27. Herrera AM, McParland BE, Bienkowska A, Tait R, Paré PD, Seow CY (2005) Sarcomeres of smooth muscle: functional characteristics and ultrastructural evidence. *J Cell Sci* 118:2381–2392
28. Van Mastrigt R, Glerum JJ (1985) Electrical stimulation of smooth muscle. *J Biomed* 7:2–8
29. Siebert T, Leichsenring K, Rode C et al (2015) Three-dimensional muscle architecture and comprehensive dynamic properties of rabbit gastrocnemius, plantaris and soleus: input for simulation studies. *PLoS ONE* 10:e0130985
30. Till O, Siebert T, Rode C, Blickhan R (2008) Characterization of isovelocity extension of activated muscle: a Hill-type model for eccentric contractions and a method for parameter determination. *J Theor Biol* 255:176–187
31. Pel JJM, Van Asselt E, Van Mastrigt R (2005) Contractile properties of inner and outer smooth muscle bundles from pig urinary detrusor. *Urol Res* 33:23–30
32. Longhurst PA, Kang J, Wein AJ, Levin RM (1990) Comparative length–tension relationship of urinary bladder strips from hamsters, rats, guinea-pigs, rabbits and cats. *Comp Biochem Physiol* 96A:221–225
33. Guilford WH, Dupuis DE, Kennedy G, Wu J, Patlak JB, Warshaw DM (1997) Smooth muscle and skeletal muscle myosins produce similar unitary forces and displacements in the laser trap. *J Biophys* 72:1006–1021
34. Ranatunga KW (1984) The force–velocity relation of rat fast- and slow-twitch muscles examined at different temperatures. *J Physiol* 351:517–529
35. Siebert T, Rode C, Herzog W, Till O, Blickhan R (2008) Nonlinearities make a difference: comparison of two common Hill-type models with real muscle. *Biol Cybern* 98:133–143
36. Böhl M, Leichsenring K, Weichert C et al (2013) Three-dimensional surface geometries of the rabbit soleus muscle during contraction: input for biomechanical modelling and its validation. *Biomech Model Mechanobiol* 12:1205–1220
37. Minekus J, van Mastrigt R (2001) Length dependence of the contractility of pig detrusor smooth muscle fibres. *Urol Res* 29:126–133
38. Gordon AM, Huxley AF, Julian FJ (1966) The variation in isometric tension with sarcomere length in vertebrate muscle fibres. *J Physiol* 184:170–192
39. Ramsey RW, Street SF (1940) The isometric length–tension diagram of isolated skeletal muscle fibers of the frog. *J Cell Comp Physiol* 15:11–34
40. Schoenberg M, Podolsky RJ (1972) Length–force relation of calcium activated muscle fibers. *Science* 176:52–54
41. Gabella G, Uvelius B (1990) Urinary bladder of rat: fine structure of normal and hypertrophic musculature. *Cell Tissue Res* 262:67–79
42. Herzog W, Kamal S, Clarke HD (1992) Myofilament lengths of cat skeletal muscle: theoretical considerations and functional implications. *J Biomech* 25:945–948
43. Mow VC, Ateshian GA, Spilker RL (1993) Biomechanics of diarthrodial joints: a review of twenty years of progress. *J Biomech Eng* 115:460–467
44. Pinniger GJ, Ranatunga KW, Offer GW (2006) Crossbridge and non-crossbridge contributions to tension in lengthening rat muscle: force-induced reversal of the power stroke. *J Physiol* 573:627–643
45. Sugi H, Tsuchiya T (1988) Stiffness changes during enhancement and deficit of isometric force by slow length changes in frog skeletal muscle fibres. *J Physiol* 407:215–229
46. Edman KA (1978) Maximum velocity of shortening in relation to sarcomere length and degree of activation of frog muscle fibres. *J Physiol* 278:9–10
47. Kosterina N, Westerblad H, Lannergren J, Eriksson A (2008) Muscular force production after concentric contraction. *J Biomech* 41:2422–2429
48. Edman KA (1975) Mechanical deactivation induced by active shortening in isolated muscle fibres of the frog. *J Physiol* 246:255–275
49. Herzog W, Leonard TR (1997) Depression of cat soleus forces following isokinetic shortening. *J Biomech* 30:865–872
50. Noble MI (1992) Enhancement of mechanical performance of striated muscle by stretch during contraction. *Exp Physiol* 77:539–552
51. Linke WA, Ivemeyer M, Olivieri N, Kolmerer B, Ruegg JC, Labeit S (1966) Towards a molecular understanding of the elasticity of titin. *J Mol Biol* 261:62–71
52. Cornachione AS, Rassier DE (2012) A non-cross-bridge, static tension is present in permeabilized skeletal muscle fibers after active force inhibition or actin extraction. *Cell Physiol* 302:C566–C574
53. Corr DT, Herzog W (2016) A cross-bridge based model of force depression: Can a single modification address both transient and steady-state behavior? *J Biomech* 5:726–734
54. Arner A, Malmqvist U (1998) Cross-bridge cycling in smooth muscle: a short review. *Acta Physiol Scand* 164:363–372
55. Maruyama K, Kimura S, Tawara H (1977) Connectin, an elastic protein. *J Biochem* 86:339–345

56. Kim K, Keller TCS (2002) Smitin, a novel smooth muscle titin-like protein, interacts with myosin filaments in vivo and in vitro. *J Cell Biol* 156:101–111
57. Powers K, Schappacher-Tilp G, Jinha A, Leonard T, Nishikawa K, Herzog W (2014) Titin force is enhanced in actively stretched skeletal muscle. *J Exp Biol* 217:3629–3636
58. Bianco P, Nagy A, Kengyel A, Szatmári D, Mártonvalfi Z, Huber T, Kellermayer MSZ (2007) Interaction forces between F-actin and titin PEVK domain measured with optical tweezers. *J Biophys* 93:2102–2109
59. Kellermayer MS, Granzier HL (1996) Calcium-dependent inhibition of in vitro thin-filament motility by native titin. *FEBS Lett* 380:281–286
60. Linke WA, Krüger M (2010) The giant protein titin as an integrator of myocyte signaling pathways. *Physiology (Bethesda)* 25:186–198
61. Joumaa V, Power GA, Hisey B, Caicedo A, Stutz J, Herzog W (2015) Effects of fiber type on force depression after active shortening in skeletal muscle. *J Biomech* 48:1687–1692
62. Yang PJ, Pham JC, Choo J, Hu JC (2013) Law of urination: all mammals empty their bladders over the same duration. *J Exp Biol* 404:4–5
63. Levin RM, Reed TP, Whitbeck C, Chichester P, Damaser M (2005) Effect of strip length on the contractile dysfunction of bladder smooth muscle after partial outlet obstruction. *Urol* 66:659–664
64. Schüssler B, Laycock J, Norton P, Stanton S (1994) Pelvic floor re-education. Principles and practice. Springer, London, pp 25–26
65. Schmitz A, Böl M (2011) On a phenomenological model for active smooth muscle contraction. *J Biomech* 44:2090–2095
66. Böl M, Schmitz A, Nowak G, Siebert T (2012) A three-dimensional chemo-mechanical continuum model for smooth muscle contraction. *J Mech Behav Biomed Mater* 13:215–229
67. Böl M, Schmitz A (2013) A coupled chemomechanical model for smooth muscle contraction. In: Holzapfel G, Kuhl E (eds) Computer models in biomechanics. From nano to macro. Springer, Dordrecht, pp 63–75